Energy Efficient Capacitive Body Channel Access Schemes for Internet of Bodies

Abeer Alamoudi, Abdulkadir Celik, Ahmed M. Eltawil
Computer, Electrical, and Mathematical Sciences and Engineering Division,
King Abdullah University of Science and Technology (KAUST), Thuwal, 23955-6900, KSA.

***Abstract*—The Internet of bodies is a network of wearable, ingestible, injectable, and implantable smart objects located in, on, and around the body. Although radio frequency (RF) systems are considered a default choice for on-body communications, which should be within <5 cm vicinity of the human body, highly radiative RF propagation unnecessarily covers several meters beyond the human body. This intuitively degrades energy efficiency, leads to interference and co-existence issues, and exposes sensitive personal data to security threats. The capacitive body channel communications (BCC) is an alternative solution that confines transmission (between 10 kHz-100 MHZ) to the human body, which is more conductive than air. Since BCC has a negligible signal leakage and lower propagation loss, it has been reported to provide better physical layer security and reach nJ/bit to pJ/bit energy efficiency. Accordingly, this paper investigates orthogonal and non-orthogonal capacitive body channel access schemes for ultra-low-power IoB nodes. We present optimal uplink and downlink power allocations in closed-form, which deliver better fairness and network lifetime than benchmark numerical solvers. For a given bandwidth and data rate requirement, We also derive the maximum affordable number of IoB nodes for both directions of orthogonal and non-orthogonal schemes.**

***Index Terms*—Wireless body area networks; Capacitive Body Channel Communication, Orthogonal Multiple Access, Non-Orthogonal Multiple Access; Power Control; and Ultra-low power IoB network.**

I. Introduction

The Internet of bodies is an imminent extension to the vast Internet of Things (IoT) ecosystem, which can be defined as a network of uniquely identifiable smart objects in, on, and around the human body [1]. Depending on their operational location, the IoB nodes can be wearable, ingestible, injectable, and implantable devices. This wide variety of IoB nodes can transform our perception of various sectors, such as patient monitoring, preventative healthcare, wellness, fitness, and cybersecurity, to name a few. Noting that IoB has its root in wireless body area networks (WBANs) [2], the IEEE 802.15.6 Standard defines physical and medium-access layer specifications to meet various quality of service (QoS) metrics such as latency, throughput, and power efficiency [3]. To this aim, the IEEE 802.15.6 Standard specifies three main wireless technologies: narrowband (NB) and ultra-wideband (UWB) radio frequency (RF) communications, and body channel communications (BCC).

The NB and UWB channels experience significantly different attenuation patterns in, on, and around the human body, which is a lossy, heterogeneous, and frequency-dependent dielectric medium. Even though RF systems are widely adopted thanks to their own virtues for in-body and off-body links, they are not the best fit for on-body communications because of their highly radiative and omnidirectional propagation nature that can cover tens of meters of space around the body. Since on-body communication should occur within the very close vicinity of the body (<5 cm), radiating RF signals with such unnecessary coverage 1) reduces energy efficiency, 2) causes interference to/from other IoB nodes, especially in crowded license-free bands, 3) and leads to security risks and privacy concerns as it inadvertently permits eavesdropping and overhearing. Moreover, NB and UWB systems require a complex and power-hungry radio front end, which reduces the node lifetime and needs a larger battery size. Indeed, all these drawbacks contradict the low-cost, miniature, and ultra-low power IoB design goals.

The BCC is an alternative form of communication that uses human skin tissues as a transmission medium and detains the signal propagation to the human body. The capacitive BCC is illustrated in Fig. 1 where signal electrodes are in touch with the skin to form the signal (forward) path, whereas the floating ground electrodes form the return (backward) path through the environment. Since the forward path encounters a milder signal fading due to the body conductivity, the channel attenuation is mainly dominated by over-the-air capacitive backward paths [4].

The BCC is specifically designated to operate between 100 kHz and 100 MHz since the human body acts as an antenna at frequencies above 100 MHz. In addition to confining signal to the human body, this operational frequency keeps the signal leakage at a very low level [5], which enhances energy efficiency and physical layer security as a result. Operating at below 100 MHZ also makes carrier less communication possible as the transceiver size can be decoupled from the carrier wavelength, eliminating the need for radio front-ends. Indeed, the capacitive BCC transceivers have shown to achieve energy efficiency levels ranging between nJ/bit to pJ/bit levels [6], [6]–[8]. Overall, the BCC is a promising technology to reach ultra-low-power, miniature, and low-cost IoB devices with better physical layer security attributes.

The recent research efforts primarily focus on channel modeling [1, and references therein] and transceiver design [6]–[8] aspects of the capacitive BCC without paying sufficient attention on communication theory and networking prospects. Therefore, this paper proposes energy-efficient orthogonal and non-orthogonal capacitive body channel access schemes to enable ultra-low-power IoB communications. We derive optimal transmission power control in closed form for both uplink (UL) and downlink (DL) IoB traffic. Compared to numerical solvers, the closed-form solutions are shown to provide

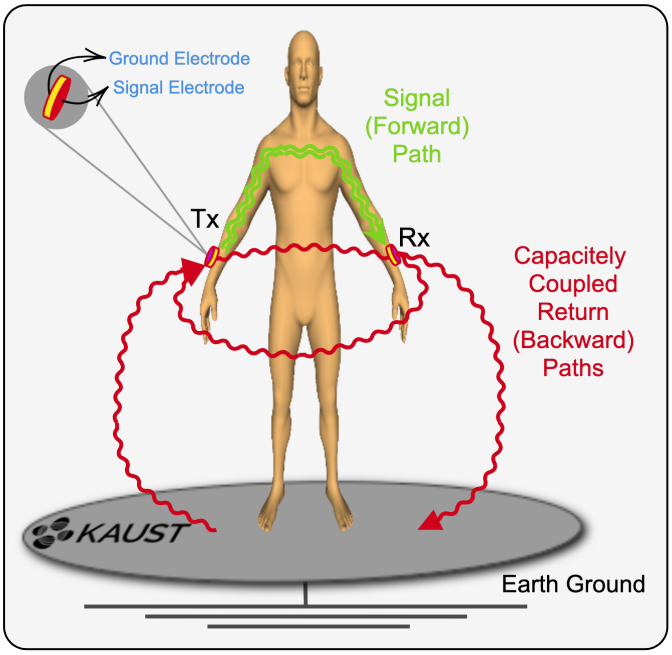

Fig. 1: Illustration of signal and return paths of capacitive body channel communications.

better fairness among IoB nodes, which enhances the IoB network lifetime substantially. For a given bandwidth and QoS requirement, we also analyze the maximum feasible number of IoB nodes for orthogonal and non-orthogonal schemes in both UL and DL directions. This analysis is fundamental to unleash the potential of BCC for supporting a seamless multi-node operation.

The remainder of the paper organized as follows: Section II presents the capacitive body channel access schemes. Section III formulates the problem and provide closed form solutions for the optimal power control. Section IV analyzes the maximum affordable number of nodes. Section V presents numerical results. Lastly, Section VI conclude the paper with a few remarks.

II. Capacitive Body Channel Access

We consider an IoB network wherein a wearable hub device (e.g., smartwatch) communicates with K on-body IoB nodes through the time-slotted uplink and downlink transmissions. The smartwatch plays the role of an access point that orchestrates the IoB network and exchanges the information with off-body entities (e.g., smartphones, base stations, routers, etc.) utilizing RF communication methods, e.g., cellular, Bluetooth, Wi-Fi, etc. We should note that the proposed methods are not limited to a specific IoB node deployment over the body, which is a function of the underlying application. Throughout the paper, we denote the total available UL and DL bandwidth for K IoB nodes, time slot duration, and thermal noise power spectral density by B, T, and N_0, respectively. Additionally, P_k and P_h symbolizes the node's and the hub's maximum transmission power, respectively. Without loss of generality, we assume that P_k and P_h are equal to P, which ensures the safety compliance of the regulatory bodies. Moreover, the reciprocal channel between n_k and n_h is represented by g_k^h g_h^h. We refer interested readers to [1] for a comprehensive survey of BCC channel models.

A. Orthogonal Multiple Access (OMA)

The OMA mitigates the multiple access interference by allocating each node with dedicated and equal bandwidths of $B\{K$ Hz. In the UL transmission, the received signal from the k^{th} node, n_k, at the hub node, n_h, on the k^{th} subband is given by

$$y_k^h \quad \sqrt{P g_k^h \, \vartheta_k^h} x_k \quad z_h; \; k \, \mathrm{P} \, K \tag{1}$$

where K denotes the index set of all IoB nodes, ϑ_k^h P r0; 1s is the power allocation weight of UL-OMA scheme, x_k is the transmit message of the k^{th} node*, z_h N p0; $N_0 B\{K$q represents the additive white Gaussian noise at n_h. Accordingly, the signal-to-noise-ratio (SNR) of UL-OMA is given by ϑ_k^h $\frac{P g_k^h \vartheta_k^h}{N_0 B\{K}$. Therefore, based on Shannon's channel capacity theorem the maximum UL achievable throughput for n_k is given by

$$\hat{R}_k^h \quad \frac{B}{K} \log_2 \; 1 \quad \vartheta_k^h \; ; k \, \mathrm{P} \, K: \tag{2}$$

In the DL transmission, the maximum transmission power of n_h is also equally divided between nodes, which yields ϑ_h^k $\frac{P g_h^k \vartheta_h^k}{N_0 B}$. Accordingly, the DL-OMA scheme can easily be obtained by replacing the terms p q_k and p q_k^h with the terms p q_h and p q_h^k in (1)-(2), respectively.

B. Non-Orthogonal Multiple Access (NOMA)

Unlike OMA, NOMA permits all IoB nodes to transmit their information concurrently over the entire bandwidth B. As a result, the UL and DL receiver nodes n_h and n_k performs multi-user detection by means of successive interference cancellation (SIC), respectively.

1) Uplink NOMA: In the UL-NOMA, the observed signal at n_h is an aggregation of the transmit signals as follows

$$y_h \quad \sum_{k \mathrm{P} K} \sqrt{P g_k^h \, !_k^h} x_k \quad z_h; \tag{3}$$

where K denotes the index set of IoB nodes arranged in ascending order of their channel gains, $!_k^h$ P r0; 1s are the UL-NOMA power allocation weights, and z_h N p0; $N_0 B$q. The UL-NOMA scheme allocates power accordingly to ensure that received powers, p_k^h $P g_k^h !_k^h; @k$, can be differentiated and follows the same ascending order, i.e.,

$$\underbrace{p_1^h \; ::: \; p_k^h}_{\text{Undecodable}} \; ::: \; \underbrace{p_K^h}_{\text{Decodable}} \tag{4}$$

Accordingly, the SIC receiver decodes and subtracts messages in descending order of their received power. In this way, the n_k can cancel interference coming from higher rank

*We will consider that all transmit messages satisfy $E\{|x_k|^2\} = 1; \forall k$, throughput the paper.

nodes while the lower rank IoB nodes' messages are regarded as interference. The SIC receiver may not cancel all the interference due to channel estimation errors and hardware limitations. In this case, the signal-to-interference-plus-noise ratio (SINR) of imperfect SIC and maximum achievable data rate are given by

$$:_k^h \quad \frac{P g_k^h !_k^h}{\sum_{i=1}^{k-1} P g_i^h !_i^h \quad \sum_{j=k+1}^{K} P g_j^h !_j^h \quad N_0 B}; \tag{5}$$

where the first term in the denominator represents the interference resulting from the decoding order's succeeding messages whereas the second term constitutes the imperfections in SIC, i.e., $\in [0,1)$ is the residual error coefficient. Accordingly, the achievable UL rate of n_k is given by

$$\dot{R}_k^h \quad B \log_2(1 + :_k^h); k \in K. \tag{6}$$

2) Downlink NOMA: In the DL-NOMA, n_h broadcasts a superimposed signal, that is a weighted summation of the intended signals intended for all nodes and received by n_k as

$$y_k \quad \sum_{k \in \hat{K}} \sqrt{P g_h^k !_h^k} x_k \quad z_k; \tag{7}$$

which is subject to total power consumption constraint, i.e., $\sum_{k \in K} !_h^k \le 1$ where $!_h^k \in [0,1)$ are the DL-NOMA power allocation weights and K denotes the index set of IoB nodes arranged in ascending order of their channel gains. Notice that the DL-NOMA follows an opposite decoding order, which yields the following SINR levels for the SIC receiver

$$:_k^h \quad \frac{P g_h^k !_h^k}{\sum_{i=1}^{k-1} P g_h^i !_h^i \quad \sum_{j=k+1}^{\hat{K}} P g_h^j !_h^j \quad N_0 B}; \tag{8}$$

Following the SIC procedure, the achievable UL rate of n_k is given by

$$\dot{R}_h^k \quad B \log_2(1 + :_h^k); k \in \hat{K}. \tag{9}$$

C. Impacts of Decoding Order on Energy Efficiency, Fairness, and Network Lifetime

The decoding order of SIC receiver has a substantial impact on energy efficiency and power consumption fairness among the nodes. In [9]–[11], it has been shown that descending and ascending channel gain ordering deliver the highest NOMA gain over OMA, respectively. Noting that these works consider maximum sum-throughput objective, reversing these orders delivers a much lower energy consumption while increasing the fairness substantially, which mainly determines the IoB network lifetime. To quantify these key performance metrics, let us first model the power consumption of IoB nodes as follows

$$P_{k;c}^{ul} \quad P_k^{crc} \quad P_k^{tx} \quad E_k^{crc} R_k^h \quad P !_k^h; \tag{10}$$

where P_k^{crc} and P_k^{tx} are the power consumed for circuit and transmission. In the BCC transceiver design literature, energy efficiency of transceivers are often measured by energy consumed per transmitted bit. Therefore, P_k^{crc} can be defined as multiplication of tranceiver efficiency, E_k^{crc} [Joules/bit], and data rate R_k^h [bps]. On the other hand, effective transmission power is simply weighted maximum transmission power, $P !_k^h$, where we omit $(\cdot)$ and $(:)$ notations to capture both UL-OMA and UL-NOMA schemes. Similarly, the power consumption of the hub is given by

$$P_c^h \quad \sum_{k=1}^{K} P_{k;c}^{dl} \quad \sum_{k=1}^{K} E_h^{crc} R_h^k \quad P !_h^k. \tag{11}$$

Accordingly, we exploit Jain's index to measure the UL power consumption fairness as follows

$$J\left(P_{1;c}^{ul}; P_{2;c}^{ul}; \ldots; P_{K;c}^{ul}\right) \quad \frac{\left(\sum_{k=1}^{K} P_{k;c}^{ul}\right)^2}{K \sum_{k=1}^{K} \left(P_{k;c}^{ul}\right)^2} \in [0,1]; \tag{12}$$

which can be rewritten for the DL case by replacing $P_{k;c}^{dl}$ with $P_{k;c}^{ul}$. Assuming that identical IoB nodes, we define the network lifetime metric as the time span between network initialization and the time slot when the first battery depletion occurred, i.e.,

$$NL \quad \min_{\forall k} \left\lfloor \frac{B_k^{int}}{!_k P_{k;c}^{ul} T} \right\rfloor; \tag{13}$$

where B_k^{int} is the initial battery level and $!_k$ is the transmission duty cycle of n_k. In Section V, we will provide a thorough numerical analysis of these performance metrics.

III. Problem Formulation and Solution Methodology

A. Problem Formulation

It is obvious from (13) the network lifetime is mainly determined by power consumptions given in (10) and (11). The optimization problem that optimizes the power allocation weights to minimize total UL power consumption can be formulated as

$$\begin{aligned} \mathbf{P_{UL}}: & \min_{\mathbf{0} \preceq \omega \preceq \mathbf{1}} \quad \sum_{k \in K} P_c^k \\ C_1: \quad & \text{s.t.} \quad R_k^h(!) \ge R_k^h, \ \forall k \end{aligned}; \tag{14}$$

where C_1 is QoS constraints that ensures that n_k is provided with a data rate not less than its demand R_k^h and $\preceq$ denotes the pairwise inequality. Similarly, the DL problem can be formulated as

$$\begin{aligned} \mathbf{P_{DL}}: & \min_{\mathbf{0} \preceq \omega \preceq \mathbf{1}} \quad P_c^h \\ C_1: \quad & \text{s.t.} \quad R_h^k(!) \ge R_k^h, \ \forall k, \\ C_2: \quad & \sum_k !_h^k \le 1 \end{aligned}; \tag{15}$$

where C_2 is an additional constraint to ensure total DL transmission power is less than the maximum transmission power of n_h. Both (14) and (15) can be put into a convex optimization problem form and solved by numerical methods. However, considering the low-cost and ultra-low-power design

goals of IoB nodes, it is necessary to derive closed-form optimal power allocations to reduce hardware cost and power consumption related to the computational complexity.

B. Solution Methodology

Both $\mathbf{P_{UL}}$ and $\mathbf{P_{DL}}$ reach optimal point when QoS constraints are active, i.e., satisfied with equality, because providing a data rate more than demanded increases both circuit and transmission power consumption. Accordingly, these problems can be rewritten as follows

$$(\mathbf{I} - \mathbf{J}\boldsymbol{\Gamma})\mathbf{p} = \boldsymbol{\sigma}; \tag{16}$$

where vectors are of size $K \times 1$, matrices are of size $K \times K$, $\mathbf{I}$ is the identity matrix, $\boldsymbol{\Gamma} = \mathrm{diag}(\gamma_1, \ldots, \gamma_k, \ldots, \gamma_K)$ is the diagonal matrix of the SINR demands corresponding to QoS demands, $\mathbf{p}$ is the column vector of the received powers, $\boldsymbol{\sigma}$ is the column vector of the receiver noise, and $\mathbf{J}$ is the interference channel gain matrix with entries

$$J_i^j = \begin{cases} 0, & i = j \\ \text{OMA}: \begin{cases} 0, & i = j \\ 0, & i \neq j \end{cases} \\ \text{UL-NOMA}: \begin{cases} \gamma_k, & i = j \\ 1, & i \neq j \end{cases} \\ \text{DL-NOMA}: \begin{cases} \gamma_k, & i = j \\ 0, & i \neq j \end{cases} \end{cases} \tag{17}$$

where entries 1, 0, and γ_k cases correspond to canceled interference (or no interference in OMA), self interference, and residual interference, respectively. Notice that (16) is subject to $p_k \geq \gamma_k g_k^h$ due to $\omega_k^h \geq 1$ in the UL. Likewise, in the Dl, (16) is also subject to $p_k \geq \gamma_k g_k^h$ due to $\gamma_k \omega_h^k \geq 1$ in addition to $p_k \geq \gamma_k g_h^k$ due to $\omega_h^k \geq 1$. Assuming that $\boldsymbol{\Gamma}$ cannot be zero in practice, $\mathbf{J}$ has non-negative elements and is generally considered to be irreducible [12].

Perron-Frobenius theorem states for a non-negative irreducible matrix that the maximum eigenvalue of $\mathbf{J}$ is real-positive and eigenvector corresponding to the maximum eigenvalue is non-negative [13]. The standard matrix theory teaches us that a feasible solution for (16) requires the necessary and sufficient condition of having magnitude of the maximum eigenvalue of $\mathbf{H} = (\mathbf{I} - \boldsymbol{\Gamma}\mathbf{J})$ to be less than unity [12]. Assuming feasible QoS demands, the solution for (16) is then given by $\mathbf{p} = (\mathbf{I} - \boldsymbol{\Gamma}\mathbf{J})^{-1}\boldsymbol{\sigma}$, from which the optimal power allocation weights can be obtained as follows:

1) OMA: Defining the SINR constraint by $\gamma_k = 2^{\frac{R_k^h K}{B}} - 1$, the optimal power allocations for UL-OMA and DL-OMA are given by

$$\omega_k^{h,*} = \frac{\gamma_k^h N_0 B}{g_k^h K P}, \forall k = K, \text{ and} \tag{18}$$

$$\omega_h^{k,*} = \frac{\gamma_k^h N_0 B}{g_k^h P}, \forall k = K, \tag{19}$$

which are subject to $\omega_k^{h,*} \geq 1, \forall k$, and $\omega_h^{k,*} \geq 1, \forall k$, respectively.

2) UL-NOMA: Defining the SINR constraint by $\gamma_k^h = 2^{\frac{R_k^h}{B}} - 1$, the optimal power allocation for the UL-NOMA is given by

$$\omega_k^{d,*} = \frac{\gamma_k^h \frac{N_0 B}{P g_k^h}}{1 - \frac{1}{1+\gamma_k^h} - \frac{1}{1+\frac{\gamma_k^h}{1+\gamma_1^h}}(K-k-1)}, \forall k = K, \tag{20}$$

which can be simplified for the perfect case ($\gamma \to 0$) as follows

$$\omega_k^{d,*} = \frac{N_0 B}{P g_k^h}(\gamma_k^h + 1)(\gamma_k^h + 1)^{K-k-1}, \forall k = K. \tag{21}$$

3) DL-NOMA: Defining the SINR constraint by $\gamma_h^k = 2^{\frac{R_h^k}{B}} - 1$, the optimal power allocation for the UL-NOMA is given by

$$\omega_1^{h,*} = \frac{\frac{1}{h}\frac{N_0 B}{P g_h^1}}{1 - \frac{1}{1+\frac{1}{h}} - \frac{1}{1+\frac{\frac{1}{h}}{1+\frac{1}{h}}}(K-1)} \tag{22}$$

$$\omega_k^{h,*} = \frac{\omega_1^{d,*}}{P g_h^k}\left(\frac{1}{1+\frac{k}{h}}\right)^{K-k}, \forall k = K. \tag{23}$$

which can be simplified for the perfect case ($\gamma \to 0$) as follows

$$\omega_d^{h,*} = \frac{N_0 B}{P g_h^k}(\gamma_k^h + 1)(\gamma_k^h + 1)^{K-k}, \forall k = K. \tag{24}$$

IV. Maximum Feasible Number of Nodes

In this section, we derive the maximum feasible number of additional nodes, $K_{\max}$, that can be admitted to the IoB network. This feasibility analysis is especially useful to understand largest network size for a given network bandwidth.

A. OMA

In the UL-OMA scheme, the optimal power allocation is violated if at least one of the nodes require a weight more than unity as per (18). Since this node is the lowest channel gain user by intuition, $K_{\max}$ can be obtained from the inequality $\frac{\gamma_k^h N_0 B}{g K P} \geq 1$, where g is the lowest channel gain in the network. For the sake of analytical tractability we assume $\gamma_k^h \gg 1$ and approximate $\gamma_k^h = 2^{\frac{R_k^h K}{B}} - 1 \approx 2^{\frac{R_k^h K}{B}}$, which yields $K_{\max}$ from above equality as

$$K_{\max} = \frac{W_{-1}\left(\frac{N_0 R}{gP}\ln(2)\, 2^{-\frac{B}{R}\ln(2)}\right)}{\ln(2) R}, \tag{25}$$

where $W_{-1}(\cdot)$ is the -1th branch of Lambert-W function. For the DL-OMA, there is no need for an approximation and $K_{\max}$ can be obtained from $\frac{\gamma_h^k N_0 B}{gP} \geq 1$ as follows

$$K_{\max} = \left\lfloor \frac{B}{R}\log_2\left(1 + \frac{Pg}{N_0 B}\right) \right\rfloor. \tag{26}$$

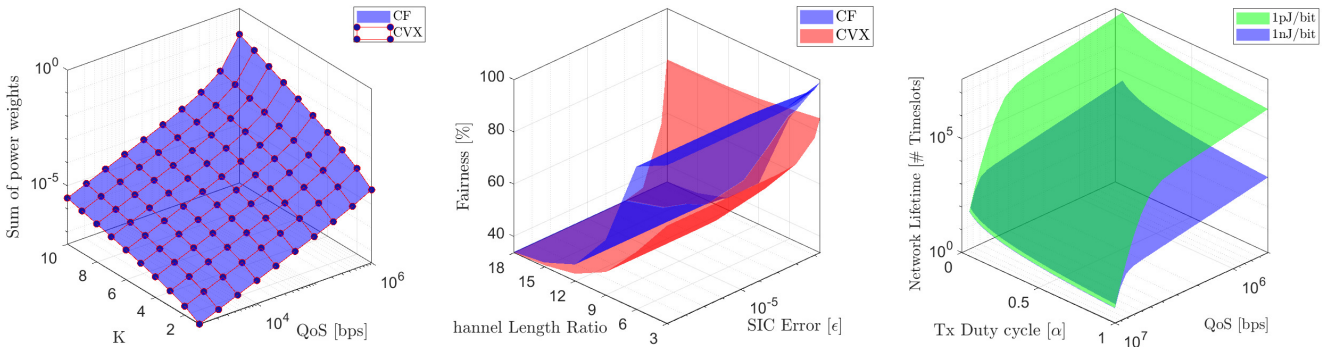

Fig. 2: Impact of various design parameters on key performance metrics: a) sum of power weights obtained by proposed CF solution and CVX w.r.t QoS and K; b) fairness comparison between proposed CF solutions and CVX w.r.t SIC and channel gain ratio; and c) network lifetime for different transceiver energy efficiencies w.r.t QoS and transmission duty cycle.

B. UL-NOMA

For the NOMA scheme, we consider perfect SIC and identical QoS requirements, R, which yields identical SINR thresholds . As per (21), the highest channel gain node is allocated with highest transmission power, which is expected to violate the power constraint first. Thus, $K_{\max}$ can be obtained from $\frac{N_0 B}{Pg}$ p 1q$^{k\ 1}$ ¤ 1 as follows

$$K_{\max} \quad 1 \quad \frac{\log \frac{Pg}{N_0 B}}{\log p1 \quad q} \quad ; \tag{27}$$

where g is the maximum channel gain in the IoB network. That is, a node with channel gain g can allow up to $K_{\max}$ 1 nodes' admission to the network.

C. DL-NOMA

On the contrary of UL-NOMA, the $K_{\max}$ can be derived from the total power weight constraint $\sum_{k\ 1}^{K} !_k$ ¤ 1. As per (21), the highest channel gain node is allocated with highest transmission power, which contributes to the total weight most. By assuming other nodes has the same highest channel gain, g, the total weight can be approximated as follows

$$\sum_{k\ 1}^{K} !_k \quad \sum_{k\ 1}^{K} p \quad 1q^K \frac{1}{p \quad 1q^k} \quad \sum_{k\ 1}^{K} a\%^k \tag{28}$$

where % $\frac{1}{p \quad 1q}$ and a % ^{K}. By setting m 。 1 and n K in the geometric progression formula, i.e., $\sum_{k\ m}^{n} a\%^k$ $a\frac{p\%^m \quad \%^{n+1}q}{1 \quad \%}$; (28) can be rewritten as

$$\sum_{k\ 1}^{K} !_k \quad \frac{\% \quad ^K p\% \quad \%^K \ ^1q}{1 \quad \%} \quad \frac{}{1 \quad \%} p\%^1 \quad ^K \quad \%q \tag{29}$$

By substituting % $\frac{1}{p \quad 1q}$ into (29), we obtain $\prod_{k\ 1}^{K} !_k$ p1 q^K 1 ¤ 1, which yields

$$K_{\max} \quad \left[\frac{\log p \frac{1}{1}q \ -}{\log p1 \quad q} \right] : \tag{30}$$

TABLE I: Simulation Parameters

Par.	Value	Par.	Value	Par.	Val.	Par.	Val.
B	1 MHz	N_0	-174 dBm/Hz	B_k^{init}	1 Joules	K	3
T	1 sec.	P_m	-30 dBm	R	1 Mbps		1

V. Numerical Results

In this section, simulation results are illustrated to assess the performance of the proposed energy-efficient body channel access schemes as we investigate various network design parameters. Unless stated otherwise, parameters available in Table I will be exploited throughout the simulations.

Fig. 2a compares the sum of power weights obtained via the proposed CF solution and CVX with respect to QoS constraints and the number of IoB nodes. It is clear from Fig. 2a that the results attained by both approaches match tightly. The total power consumption increases with QoS demands and network size. Fig. 2b also shows that CF surpasses CVX in terms of fair power allocation between IoB nodes with respect to cancellation error and ratio of channel lengths $\grave{}_3^h\{\grave{}_1^h$. In both cases the fairness reduces as we push n_3 further away from the hub. Interestingly, the fairness metric reaches the maximum value in both CF and CVX as Ñ 1 because 1 yields an interference OMA network, where all nodes transmit at maximum power without power control. Nonetheless, this fairness does not necessarily imply energy efficiency as 1 also yields the higher power consumption. Moreover, the impact of channel length ratio $\grave{}_3^h\{\grave{}_1^h$ at 1 reduces fairness drastically for CF unlike CVX. Lastly, Fig. 2c shows the network lifetime of identical nodes with respect to the transmission duty cycle and QoS demands. Since a considerable amount of energy is consumed by the circuit, we look at two different transceiver energy efficiencies. In both cases, the results agree with the intuition that lower values (i.e., lower energy departure rate) and lower QoS demand results in a longer lifespan. Moreover, deploying a transceiver with 1 pJ/bit energy efficiency will increase the life span by 10^3 slots compared to 1 nJ/bit. That is, the overall